World Academy of Science, Engineering and Technology
International Journal of Mechanical and Mechatronics Engineering
Vol:5, No:6, 2011

# Study of Real Gas Behavior in a Single-Stage Gas Gun

A. Moradi[1], S. Khodadadiyan[2]

***Abstract*—**In this paper, one-dimensional analysis of flow in a single-stage gas gun is conducted. The compressible inviscid flow equations are numerically solved by the second-order Roe TVD method, by using moving boundaries. For investigation of real gas effect the Noble-Able equation is applied. The numerical results are compared with the experimental data to validate the numerical scheme. The results show that with using the Noble-Able equation, the muzzle velocity decreases.

***Keywords*—**Gas gun, Roe, projectile, muzzle velocity



## I. Introduction

A number of different methods can be used to launch a projectile at a high velocity exceeding a few kilometers per second. Many years ago, two types of single-stage gas guns were in general used: powder gun using the standard gunpowder as the propellant, and gas gun using the compressed gas as the propellant. A powder gun with a reasonably large caliber launches a projectile with a maximum velocity of about 2-2.2 km/s. A single-stage gas gun using light gas such as helium or hydrogen as the propellant provides increased projectile velocity. In such powder guns the projectile is driven by gas from the burning gun powder, as well as the principle of a other single-stage gas gun is that gas, initially stored at high pressure, is suddenly released and allowed to act on the rear face of a projectile enclosed inside a long tube or barrel. The gas pressure difference across the projectile causes it to accelerate along the barrel until emerging from the muzzle. Jacobs [1] presented a report about shock tube modeling with a light gas gun. He estimate the performance of a free piston driven impulse facility, and in his report the presented a simple formula for calculating the friction between the projectile and the barrel wall. Of course, in majority of researches has been ignored the concepts of the sliding friction in the conventional gas gun. Sasoh et al. [2] investigated projectile acceleration in a single-stage gas gun at breech pressures below 50 MPa experimentally. Nussbaum et al. [3] used the one dimensional numerical solution for gas particle flows with combustion in the powder gun. They applied the first-order TVD Rusonov scheme for simulation of the powder gun and to validate their results, they compared numerical results with other reported results. Yingxing et al. [4] performed a characteristics study on performance of a two -stage light gas gun. They used the van der waals model for equation of state. Kashimov et al. [5] proposed an improved procedure for modeling the operation of light gas gun. The motion of the projectile in both the firing chamber and the light-gas chamber is studied as well. Jahnston and Krishnamoorthy [6] used the one dimensional Godunov method to solve the governing equations system. They used the experimental data for validating results. Philippon et al. [7] implemented an experimental study on the friction at high sliding velocities. Jiang et al. [8] investigated blast flow fields induced by a high-speed projectile in the barrel of a gas gun. They used the commercial CFD-FASTRAN finite volume solver package for the axisymmetric numerical simulation. They compared the numerical and experimental results in order to validate their research. Jiang et al. [9] investigated shocked flow induced by supersonic projectiles moving in the tubes.

Most of the previous researches have not investigated the effect of real gas model in simulation of a gas gun. They applied ideal gas model for simulation of the flow in a gas gun. While in this paper, the Noble-Able equation is selected for the equation of state. Here, the transonic and supersonic gas guns with 265 mm and 50 mm bore respectively are investigated and discussed. For more information about transonic gas gun refer to Ref [6].

## II. The Governing Equations

Quasi-one-dimensional flow governing equation can be expressed as

$$\frac{\partial(S\vec{\mathbf{U}})}{\partial t}+\frac{\partial\vec{\mathbf{f}}}{\partial x}-\vec{\mathbf{H}}=0 \tag{1}$$

where, $S$ is cross section area, and conservative variables $\vec{\mathbf{U}}$, inviscid flux $\vec{\mathbf{f}}$ and source term $\vec{\mathbf{H}}$ are defined as

$$\begin{aligned}\vec{\mathbf{U}}&=(\rho,\rho u,\rho e_t)^T\\ \vec{\mathbf{f}}&=S(\rho u,\rho u^2+p,(\rho e_t+p)u)^T\\ \vec{\mathbf{H}}&=\frac{dS}{dx}(0,p,0)^T\end{aligned} \tag{2}$$

where, $\rho$, $u$, $p$ and $e$ are the density, the velocity, the static pressure and the total energy per mass, respectively. The cross section area is assumed constant, so that (1) can be write as

$$\frac{\partial\vec{\mathbf{U}}}{\partial t}+\frac{\partial\vec{\mathbf{f}}}{\partial x}=0 \tag{3}$$

1. A. Moradi is Master of Science's Student, Department of Mechanical Engineering, Bu Ali Sina University, Hamedan, Iran (phone: +98(861) 3131736; fax: +98(861)4131217; E-mail: amirmoradi_hs@yahoo.com).

2. S. Khodadadiyan is Master of Science's Student, Department of Mechanical Engineering, Bu Ali Sina University, Hamedan, Iran. (E-mail: Skhodadadiyan@gmail.com).

The pressure is related with the equation of state for the Noble-Able equation given by

$$p = \frac{(\gamma - 1)\rho e}{(1 - \eta\rho)} \tag{4}$$

Where $\eta$ is the gas covolume. The total energy $e_t$ is defined as

$$e_t = e + \frac{1}{2}u^2 \tag{5}$$

## III. Numerical Simulation

In this paper, the second semi-discretized TVD Roe scheme is used for solving (3) which is expressed as [10]:

$$\mathbf{U}_i^{n+1} = \mathbf{U}_i^n - \frac{\Delta t}{\Delta x}(\mathbf{f}_{i+1/2}^{*(2)} - \mathbf{f}_{i-1/2}^{*(2)}) \tag{6}$$

where $\mathbf{f}_{i+1/2}^{*(2)}$ can be expressed as

$$\mathbf{f}_{i+1/2}^{*(2)} = \mathbf{f}_{i+1/2}^{*(R)} + \frac{1}{2}\Psi(\mathbf{r}_{i-1/2}^{+})(\mathbf{f}_i - \mathbf{f}_{i-1/2}^{*(R)}) - \frac{1}{2}\Psi(\mathbf{r}_{i+3/2}^{-})(\mathbf{f}_{i+1} - \mathbf{f}_{i+3/2}^{*(R)}) \tag{7}$$

where $\mathbf{f}_{i+1/2}^{*(R)}$ is the numerical flux of the Roe scheme for a scalar conservation law, which is given by

$$\mathbf{f}_{i+1/2}^{*(R)} = \frac{1}{2}(\mathbf{f}_i + \mathbf{f}_{i+1}) - \frac{1}{2}\sum_{j=1}^{3}\left|(\lambda_{i+1/2}^{*})_j\right|(\delta\omega_{i+1/2})_j(\mathbf{r}_{i+1/2}^{*})_j, \tag{8}$$

and variables of limiter function are defined as

$$\mathbf{r}_{i-1/2}^{+} = \frac{\mathbf{f}_{i+1} - \mathbf{f}_{i+1/2}^{*(R)}}{\mathbf{f}_i - \mathbf{f}_{i-1/2}^{*(R)}} \qquad \mathbf{r}_{i+3/2}^{-} = \frac{\mathbf{f}_i - \mathbf{f}_{i+1/2}^{*(R)}}{\mathbf{f}_{i+1} - \mathbf{f}_{i+3/2}^{*(R)}} \tag{9}$$

In equation (6) $\Delta t$ and $\Delta x$ are time and space step respectively. $\Psi$ is the limiter function that has been used the Osprey limiter function [11] here. For how to calculating $\delta\omega_{i+1/2}$ and $\mathbf{r}_{i+1/2}^{*}$ for real gas model, the primitive variable vector $\vec{\mathbf{v}}$ is defined as follow

$$\vec{\mathbf{v}} = (\rho, u, p)^T \tag{10}$$

The Jacobian Matrix $\tilde{\mathbf{A}} = \frac{\partial\vec{\mathbf{f}}}{\partial\vec{\mathbf{v}}}$ is in the following form [10]:

$$\tilde{\mathbf{A}} = \begin{bmatrix} u & \rho & 0 \\ 0 & u & \frac{1}{\rho} \\ 0 & \rho c^2 & u \end{bmatrix} \tag{11}$$

The eigenvalues of the Jacobian Matrix $\tilde{\mathbf{A}}$ are:

$$\lambda_1 = u \qquad \lambda_2 = u + a \qquad \lambda_3 = u - a \tag{12}$$

where *a* is the sound speed.

The two matrixes $\mathbf{L}^{-1}$ and $\mathbf{L}$ are defined as:

$$\mathbf{L} = \begin{bmatrix} 1 & \frac{\rho}{2c} & -\frac{\rho}{2c} \\ 0 & \frac{1}{2} & \frac{1}{2} \\ 0 & \frac{\rho c}{2} & -\frac{\rho c}{2} \end{bmatrix} \qquad \mathbf{L}^{-1} = \begin{bmatrix} 1 & 0 & -\frac{1}{c^2} \\ 0 & 1 & \frac{1}{\rho c} \\ 0 & 1 & -\frac{1}{\rho c} \end{bmatrix} \tag{13}$$

Note that the columns of $\mathbf{L}^{-1}$ and $\mathbf{L}$ are the left and right eigenvectors of $\tilde{\mathbf{A}}$. The Matrix $\vec{\mathbf{M}}$ for the real gas model is defined as:

$$\mathbf{M} = \begin{bmatrix} 1 & 0 & 0 \\ u & \rho & 0 \\ \frac{u^2}{2} & \rho u & \frac{(1-\eta\rho)}{\gamma - 1} \end{bmatrix} \tag{14}$$

The Matrix $\mathbf{P}$ is given by:

$$\mathbf{P} = \mathbf{ML} = \begin{bmatrix} 1 & \frac{\rho}{2c} & -\frac{\rho}{2c} \\ u & \frac{\rho}{2c}(u+c) & -\frac{\rho}{2c}(u-c) \\ \frac{u^2}{2} & \frac{\rho}{2c}(\frac{u^2}{2} + uc + \frac{c^2(1-\eta\rho)}{\gamma-1}) & -\frac{\rho}{2c}(\frac{u^2}{2} - uc + \frac{c^2(1-\eta\rho)}{\gamma-1}) \end{bmatrix} \tag{15}$$

where $\mathbf{p}$ is the Matrix that the columns of it are the eigenvectors of Jacobian Matrix $\mathbf{A} = \frac{\partial\vec{\mathbf{f}}}{\partial\vec{\mathbf{U}}}$. The wave length vector $\delta\omega$ in (8) is defined as [10]:

$$\begin{aligned} \delta\omega &= \mathbf{L}^{-1}\delta\vec{\mathbf{v}} \\ (\delta\omega_{i+1/2})_1 &= \delta\rho_{i+1/2} - \frac{\delta p_{i+1/2}}{(a_{i+1/2}^{*})^2} \\ (\delta\omega_{i+1/2})_2 &= \delta u_{i+1/2} + \frac{\delta p_{i+1/2}}{\rho_{i+1/2}a_{i+1/2}^{*}} \\ (\delta\omega_{i+1/2})_3 &= \delta u_{i+1/2} - \frac{\delta p_{i+1/2}}{\rho_{i+1/2}a_{i+1/2}^{*}} \\ \delta z_{i+1/2} &= z_{i+1} - z_i, \end{aligned} \tag{16}$$

and the osprey limiter function is given by [11]:

$$\Psi(r) = \frac{1.5r^2 + r}{r^2 + r + 1} \tag{17}$$

## IV. The Employed Boundary Conditions

To simulate moving projectile, we must trace the moving surfaces of the projectile in each moment of solution time. This means that, in each moment of solution time, the position of the front and back sides of the projectile must be identified. For more explanations see Fig 1. The amount of velocity *u*, in point *a*, inside the projectile is interpolated the right-hand side points of the projectile, so as to the velocity of right-hand face must be exactly equal to the velocity of the projectile. The pressure and density gradients on these surfaces are considered equal zero (these conditions are due to boundary layer assumption). On the other hands, the velocity of *a* and *b* points is equal to $a_1$ (Fig. 1). Actually, by this work the right-hand side face and two cells in two sides of this surface (front and back of it) will have the same velocity and we will not have any mass fluxes in this face and the condition of solid bodyis satisfied. These boundary conditions are applied on left-hand side of the projectile similar to right-hand side of it. Our goal to apply these conditions is being entered no mass to the

projectile limit, so the simulation for moving projectile as a solid moving body is true. The interior points of the projectile are considered in to similar manner to other points of solution domain. Actually, the interior points of the projectile (except projectile boundary points) are not important here.

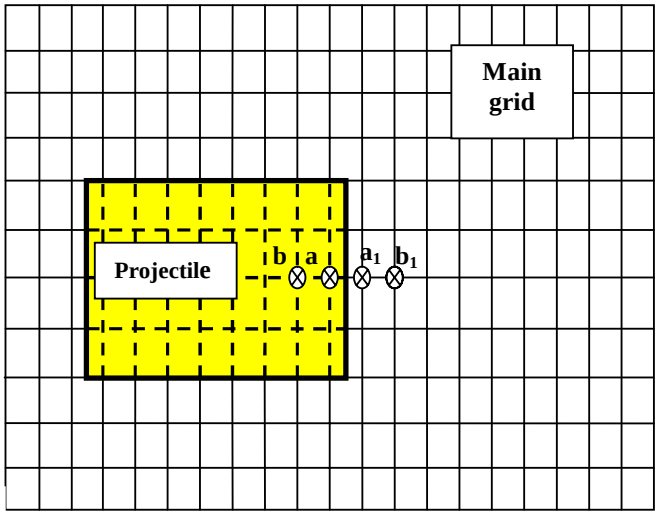


Fig. 1 Manner of data giving into points of projectile

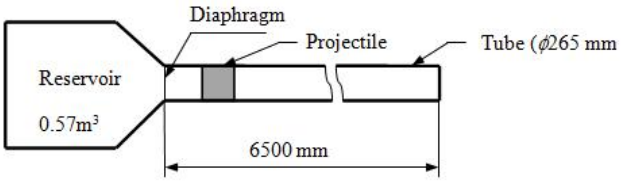


Fig. 2 The physical dimensions of single-stage transonic gas gun

## V. Results and Discussion

The transonic and supersonic single-stage gas gun with 265mm and 50 mm caliber, 6.5m and 12m tube length respectively are considered and studied in this paper. The physical dimensions of the transonic gas gun are shown in Fig. 2. The propellant gas for the transonic gas gun is nitrogen which is cooled up to 283*K*. The ambient pressure and temperature are 1*atm* and 300*K* respectively. The projectile velocity for different space steps for ideal gas model is shown in Fig. 3 where the reservoir pressure is 4*MPa* and $m_p = 27kg$ .

Fig. 3 shows that the numerical solution would be independence from space step for $\Delta x = 0.01$ . The effect of the reservoir pressure on the projectile velocity for ideal gas model is depicted in Fig. 4.

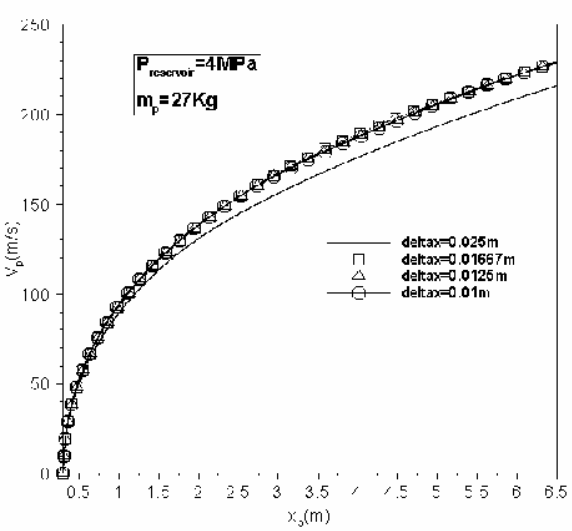


Fig. 3 Variation of projectile velocity with for different space steps for $p_{reservoir}$= 4*MPa* and $m_p$=27

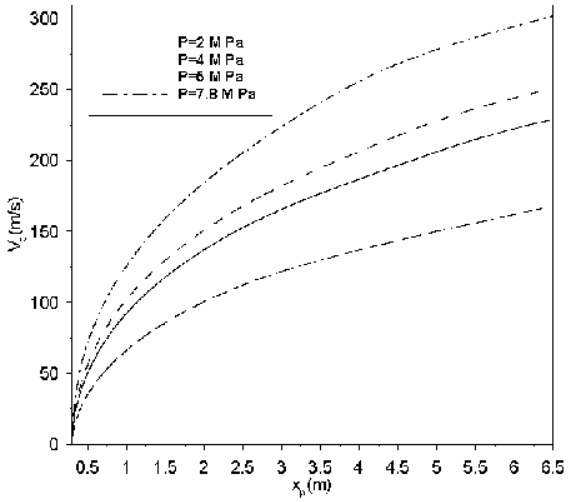


Fig. 4 The effect of reservoir pressure on the muzzle velocity for transonic gas gun with $m_p$= 27*Kg*

As expected, an increase is found in muzzle velocity with increased in reservoir pressure. The variation of projectile velocity and comparison between ideal and real gas model for reservoir pressure 4*MPa* is shown in Fig. 5. This comparison shows that for the real gas model the muzzle velocity is lower than the ideal gas one.

The analytical formula which is used for obtaining the muzzle velocity with the isentropic approximation and ideal gas equation of state is defined as:

$$\frac{dV_p}{dt} = \frac{A_p}{m_p}\left[ P_B\left(1-\frac{(\gamma_B-1)}{2a_B}V_p\right)^{\frac{2\gamma_B}{\gamma_B-1}} - P_F\left(1+\frac{(\gamma_F-1)}{2a_F}V_p\right)^{\frac{2\gamma_F}{\gamma_F-1}}\right] \qquad (18)$$

where subscript *B* and *F*, denoted the back and front side of the projectile, $\gamma$ and $a$ are the specific heat ratio and velocity of sound respectively, (18) can be solved numerically.

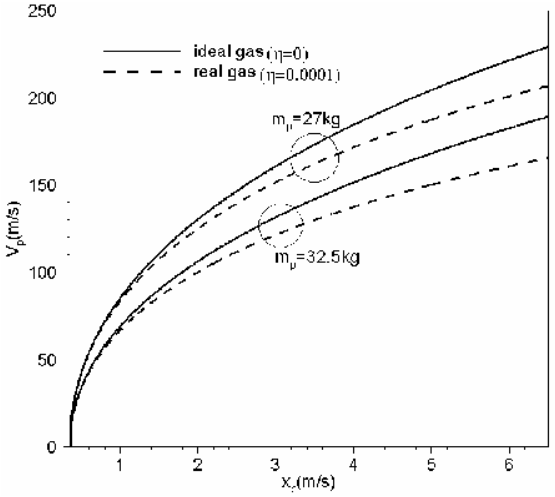


Fig. 5 Variation of the projectile velocity for different projectile mass in transonic gas gun

The propellant gas for the supersonic gas gun is helium with initial temperature 300*K*. The effect of the reservoir pressure and projected mass on the muzzle velocity for the supersonic gas gun is shown in Figs. 6 and 7 respectively.

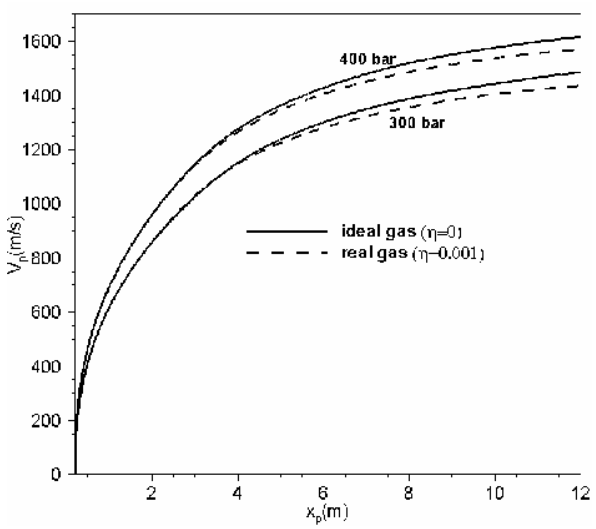


Fig. 6 Variation of the projectile velocity with reservoir pressure for supersonic gas gun when $m_p = 0.1Kg$

In the Fig. 7 is used the ideal gas equation for simulation of flow. In the supersonic gas gun, the muzzle velocity decreases with using real gas model as well. The result of comparison between numerical, analytical and experimental results for the transonic gas gun is shown in Table 1. It is evident from Table 1, the numerical results are in good agreement with that measured by experiment [6]. It is observed that discrepancy between the analytical and experimental results is evident. These results describe that the analytical data are not credible for simulation and design of a gas gun.

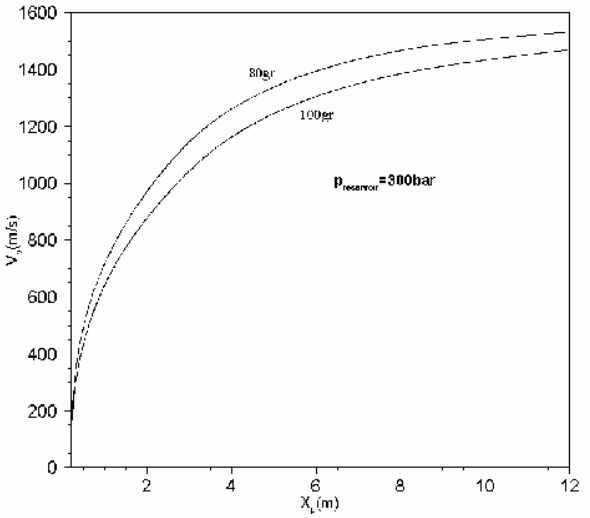


Fig. 7 Variation of the projectile velocity with projectile mass for the supersonic gas gun when $m_p = 0.1Kg$

TABLE I
COMPARISON BETWEEN EXPERIMENTAL, NUMERICAL AND ANALYTICAL RESULTS FOR TRANSONIC GUN

| $p_{reservoir}$ (MPa) | Projected mass(Kg) | Experimental $V_p$(m/s)[6] | Numerical $V_p$(m/s) (ideal gas) | Analytical $V_p$(m/s) |
|---|---|---|---|---|
| 4.0 | 27.0 | 231 | 229 | 219 |
| 4.0 | 32.5 | 216 | 213 | 205 |
| 4.0 | 42.5 | 199 | 194 | 186 |
| 5.0 | 27.0 | 252 | 250 | 239 |
| 7.8 | 27.0 | 305 | 301 | 280 |

In this paper, the results show that the one dimensional simulation and inviscid flow approximation is enough for obtaining the higher accuracy solution and the second-order Roe TVD scheme is a powerful method to simulate the subsonic and supersonic flows as well. The supersonic gas gun results indicate that obtaining high muzzle velocity about 1500 *m/s* is possible for the low weight projectile with a single-stage gas gun with helium as a propellant gas.

## VI. CONCLUSION

In this paper, the simulation of flow in a subsonic and supersonic gas guns was studied. The governing equations were solved numerically by the second-order Roe TVD scheme. The osprey limiter function was applied to obtain high accuracy solution. To verify the accuracy of the computer code, the calculated muzzle velocities were compared with the experimental results [6]. This comparison shows that there is an excellent agreement between the numerical and experimental results. The results indicate that the second-order Roe TVD scheme has a high ability to simulate the unsteady and compressible flows with low and high Mach number.

## REFERENCES

[1] Jacobs P. A., Shock tube modeling with L1d, Research Report 13/98, Department of Mechanical Engineering, University of Queensland. 1998.

[2] Sasoh A. and Ohba S. and Takayama, K., Projectile acceleration in a single-stage gun at breech pressure below 500 MPa, *Shock Waves*, vol.10, 2000, pp. 235-240.
[3] Nussbaum J. and Helluy P. and Herard J. M. and Carriere A., Numerical solution of gas-particle flows with combustion, *Flow Turbulence Combust*, vol. 76, 2006, pp. 403-417.
[4] Yingxiang W. and Zhichu Z. and Kupschus P., A characteristics study on the performance of a two- stage light gas gun, *SCIENCE IN CHINA (Series A)*, vol. 38, No. 9, 1995, pp. 1070-1082.
[5] Kashimov V. Z. and Ushakova O. V. and Khomenko P. Numerical modeling of interior ballistics processes in light gas gun, J. Appl. Mech. Tech. Phys., vol. 44 No. 5, 2003, pp. 612-619.
[6] Johnston, I. A. and Krishnamoorthy L. V., A Numerical Solution of Gas Gun Performance, DSTO-TN-0804, AR-014-105, 2008.
[7] Philippon S. and Sutter G. and Molinari A., An experimental study of friction at high sliding velocities, *Wear*, vol. 257, 2004, pp. 777-784.
[8] Jiang X. and Chen Z. and Fan B. and Li H., Numerical simulation of blast flow fields induced by a high-speed projectile, *Shock Waves*, vol. 18, 2008, pp. 205-212.
[9] Jiang Z. and Huang Y. and Takayama K., Shocked flow induced by supersonic projectiles moving in tubes, *Computers & Fluids*, vol. 33, 2004, pp. 953-966.
[10] Hirsch C., *Numerical Computation of Internal and External Flows. Vol. 2, Computational Methods for Inviscid and Viscous Flows*, John Wiley and Sons: Toronto, 1989.
[11] Waterson N. P. and Deconinck H., A Unified Approach to the Design and Application of Bounded High-order Convection Schemes, *Proceeding of 9th International Conference on Numerical Methods in Laminar and Turbulent Flow*, Pineridge Press, Swansea, 1995.